p-ISSN 2460-0768 e-ISSN 2597-6044
GeoEco, Vol. 12, No 2. July 2026 Page. 567 - 591
https://doi.org/10.20961/ge.v12i2.106740
https://jurnal.uns.ac.id/GeoEco/article/view/106740

TEMPORAL VARIATION OF VEGETATION INDEX RELATED TO PRECIPITATION DYNAMICS IN FORESTED AREA OF BOJONEGORO REGENCY

Heri Mulyanti*, Oktavianus Cahya Anggara, Bagus Saputra, Nabila Nalalizza, Eka Luluk Fitriani
Department of Environmental Science, Faculty of Science and Engineering, Universitas Bojonegoro, Bojonegoro, Indonesia

E-mail: herimulyanti.unigoro@gmail.com

ARTICLE INFO

Article History
Received : 23/07/2025
Revised : 25/12/2025
Accepted : 06/05/2026

Citation:
Mulyati, H., Anggara, O.C., Saputra, B., Nalalizza, N., and Fitriani, E.L., (2026). Temporal Variation of Vegetation Index Related to Precipitation Dynamics In Forested Area of Bojonegoro Regency. GeoEco. Vol. 12, No. 2.

ABSTRACT

Vegetation dynamics in monsoonal regions are related to climate variability, particularly precipitation. Changes in precipitation may be reflected in vegetation conditions, yet studies on the temporal relationship between NDVI and Rainfall at the regional scale remain limited. This study aims to analyze NDVI dynamics and their relationship with precipitation in Bojonegoro Regency, East Java, during 2001–2023. Using Landsat satellite imagery and CHIRPS precipitation data, the Normalized Difference Vegetation Index (NDVI) was analyzed to evaluate seasonal and interannual vegetation patterns. NDVI values were calculated for April–May and October, representing the end and beginning of the rainy season. Results show that NDVI tends to be higher at the end of the rainy season, with a median value of 0.365, compared to 0.254 at the beginning. The highest NDVI was recorded in 2021, with a median of 0.596. Forested areas demonstrated greater resilience to climate variability than croplands or degraded land. NDVI and Rainfall exhibited a complex relationship, with significant correlations observed only in 2001 at lags –2, –1, and +2. The lag time responses of NDVI after specified precipitation can be used for forest management and planting. The analysis suggests that detailed assessments using time series data are necessary for a clearer understanding. NDVI alone is insufficient, and field validation is required to confirm satellite-based interpretations. Therefore, planned management required to enhance ecosystem resilience to climate change.

Keywords: *drought; forest; lag time; NDVI; precipitation*

INTRODUCTION

Indonesia is one of the world's most forested countries, providing essential ecological services and supporting biodiversity. However, Global Forest Watch (Hansen et al., 2013) stated that approximately 10.7 Mha of primary forest in Indonesia was lost in 2024. Deforestation and forest degradation disrupt ecosystem functions, leading to adverse consequences for human and environmental health. Forest degradation also changes ecosystems, biodiversity, and ecosystem services (Weiskopf et al., 2020).

Forest cover changes trigger microclimatic shifts, including temperature rise and changes in precipitation patterns. Study found that tropical deforestation reduces precipitation by approximately 0.1 mm/month (Smith et al., 2023). Furthermore, the adverse consequences of forest change negatively impact agricultural productivity (Lawrence & Vandecar, 2015). In the Amazon, precipitation patterns closely correlate with deforestation extent, as increased land-use changes lead to higher temperatures and reduced Rainfall (Carvalho et al., 2020). Beyond meteorological impacts, deforestation is also influenced by land cover and hydrological processes, including surface runoff dynamics (Ma et al., 2024). These factors interact with precipitation and affect vegetation response at the regional scale.

Bojonegoro Regency has an extensive forested area in the southern region. These areas are primarily covered by teak forests that play a crucial role in ecosystem stability, slope stability, and recharge areas. However, forest loss is particularly pronounced in the southern sub-districts. Data from Global Forest Watch reveal that approximately 5.98 kha (-7.7%) of net vegetation cover was reduced between 2001 and 2020 (Hansen et al., 2013). A study showed that forest cover in East Java has reduced by 8% (Marga et al., 2024). Given the vulnerability of this region to drought (Mulyanti, 2023), forest loss may cause a severe impact.

Previous studies show that NDVI is influenced by precipitation and temperature (Carvalho et al., 2020; Ma et al., 2024; Smith et al., 2023). On the other hand, climate variability such as drought caused significant NDVI reduction (Hossain & Li, 2021; Jiang et al., 2024; Vicente-Serrano et al., 2020). However, most studies use aggregated or large-scale data, so regional variation is not clearly captured. Vegetation response may differ at the local scale, especially in monsoonal regions.

Temporal relationship between precipitation and NDVI is often conducted for a specific month. However, potential lag effects are not examined clearly. Vegetation does not respond instantly to Rainfall, and a delayed response may occur. This condition is still not well explained.

Therefore, a regional analysis that considers lag effects is needed to explain NDVI dynamics under precipitation variability better better. The study aims to: (i) analyse NDVI dynamics in Bojonegoro Regency in different seasons and (ii) examine the relationship between NDVI and monthly precipitation. The findings provide crucial data to support policymakers in developing more effective forest conservation and restoration strategies.

MATERIALS AND METHODS

The research focused on Bojonegoro Regency, East Java, which comprised 28 sub-districts and 419 villages. The region was located between 111°25' E – 112°09' E and 6°59' S – 7°37' S, with the Bengawan Solo River flowing through its northern section. Bojonegoro Regency was one of Indonesia's major teak-producing areas. However, forest conversion and degraded forests posed a significant challenge. Degraded forests increase vulnerability to landslides, flash floods, groundwater depletion, and biodiversity loss.

Landsat, a long-term Earth observation mission by NASA, provides systematic land-cover data. The study utilised Landsat 8 images for the years 2001, 2013, 2018, 2021, and 2023. Landsat 8 included two sensors: the Operational Land Imager (OLI) and the Thermal Infrared Sensor (TIRS). Band 3 (green) and Band 4 (Red) of the OLI sensor were used for vegetation assessment. Due to data gaps in 2001 and 2020 and systematic error in 2020, the analysis incorporated Landsat 7 Enhanced Thematic Mapper Plus (Landsat Science Outreach Team, 2023). Cloud cover was restricted to a maximum of 10% to ensure data quality. Prior to analysis, atmospheric correction was applied using the Semi-Automatic Classification Plugin in QGIS 3.14 (Congedo, 2021).

The difference between natural color (true color), infrared, and modified color (False Color 7-5-3) from Landsat 8 OLI-TIRS was illustrated in **Figure 1a**. The northern region consists of rivers, settlements, and wetlands. These wetlands are irrigated areas with easy water access. This region is difficult to identify using only a single infrared band combination, as infrared reflectance is similar for both forest cover and short vegetation (e.g., rice fields), as seen in **Figure 1b**.

The 7-5-3 band combination (**Figure 2**) enhances differentiation between wet rice fields and water bodies. Wet fields

p-ISSN 2460-0768 e-ISSN 2597-6044
https://doi.org/10.20961/ge.v12i2.106740

reflect blue, whereas water bodies absorb almost all wavelengths, appearing black. Meanwhile, forests reflect green. Short vegetation submerged in water appears dark green, blending green and black. Open land with limestone soil appears white, while built-up areas appear pink. Built-up areas are clearly distinguishable from open land. Natural and infrared composites struggle to differentiate settlements from open land, especially in areas with earthen roofs.

The 7-5-3 combination outperforms natural and infrared composites in distinguishing features in Bojonegoro Regency.

Overall, Bojonegoro Regency in May consists of multiple land cover types. Wet rice fields are distributed along the river, while settlements are concentrated along main roads, particularly in the northern central region (urban area). The eastern region contains limestone-dominated soils, appearing white in imagery. Forests dominate the southern region.

Figure 1b highlights the necessity of distinguishing southern forest cover from short vegetation to prevent false detection. A paddy field at peak growth can reflect a greener color than taller trees. To avoid false detection, forest cover is classified separately from other vegetation. Vegetation analysis was conducted for May or October, representing the end and beginning of the rainy season. April or May was used for NDVI analysis in 2001, 2018, 2020, and 2021. However, October was selected for 2013. Due to Bojonegoro's climate (Mulyanti, 2022), dry months (June-September) were excluded from the analysis.

Monthly precipitation data were obtained from the Climate Hazards Group InfraRed Precipitation with Station data (CHIRPS), which provides high-resolution (0.05° × 0.05°) gridded rainfall estimates corrected using ground-based station data (Funk et al., 2015). **Figure 3** shows precipitation grid cells over forest plantations. The selected area for NDVI-precipitation analysis is restricted to forest cover, as short vegetation can exhibit high NDVI values during peak growth phases. The selected area of interest (AOI) represents the intersection between forest cover and corrected CHIRPS precipitation grids. The analysis included 36 grids (**Figure 4**).

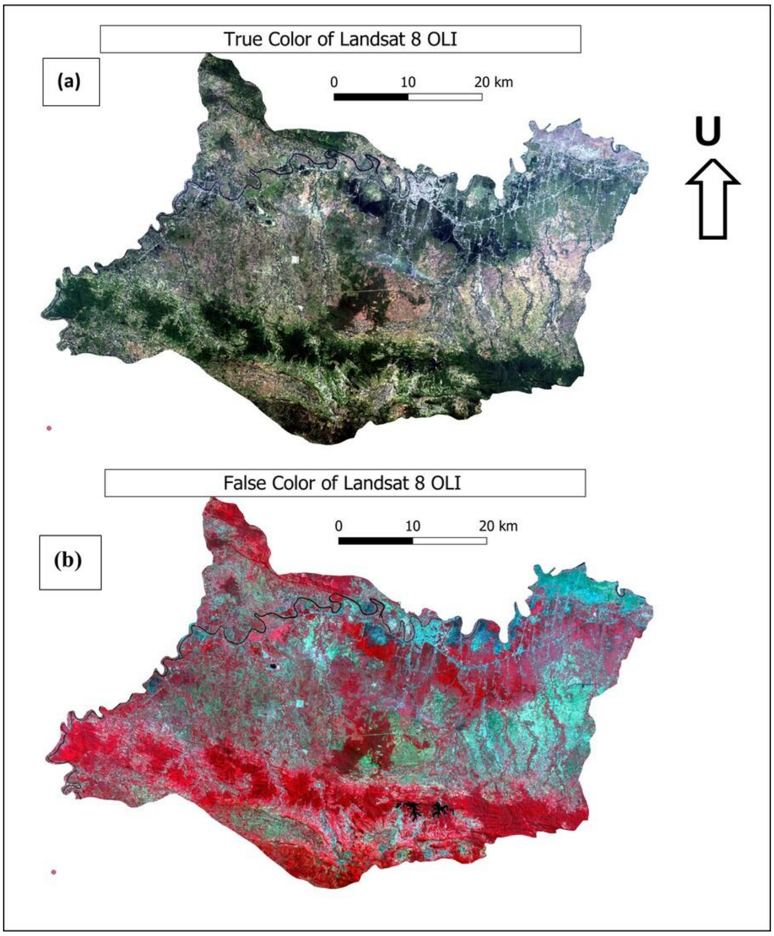

Figure 1. The Landsat 8 OLI satellite imagery for Bojonegoro Regency in 2023. (a) Natural color combination (4-3-2) and (b) Infrared band combination (5-4-3).
Source: Authors' processing (2024)

As illustrated in **Figure 4**, forests are concentrated in the southern region, with 33 grids, while the northern region contains only 3 grids with limited coverage. The northern forests are fragments of the larger Randublatung formation, which originated in the Tertiary Period and consist of clay with an anticlinal geological structure.

The NDVI was calculated based on the reflectance values from near-infrared (NIR) and red bands:

$$NDVI = \frac{(NIR - Red)}{(NIR + Red)} \quad (1)$$

where NDVI is Vegetation Index (-1 to +1 scale), NIR is Near-infrared reflectance, and Red is red band reflectance.

NDVI represents vegetation greenness and does not directly correspond to land use classes. In this study, the analysis focuses on forested areas; therefore, land use data cannot be used to validate

NDVI values. NDVI is used to capture relative changes in vegetation condition rather than absolute vegetation status. The observed NDVI patterns follow seasonal rainfall variability, which supports the interpretation of vegetation dynamics. Direct validation using field observation or in situ vegetation measurements is not conducted.

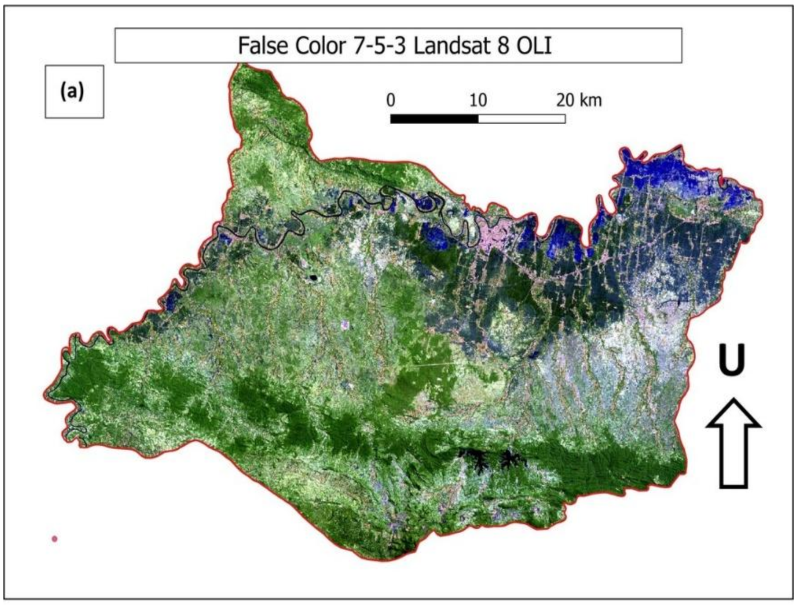

Figure 2. Landsat 8 OLI imagery using the 7-5-3 band combination.
Source: Authors' processing (2024)

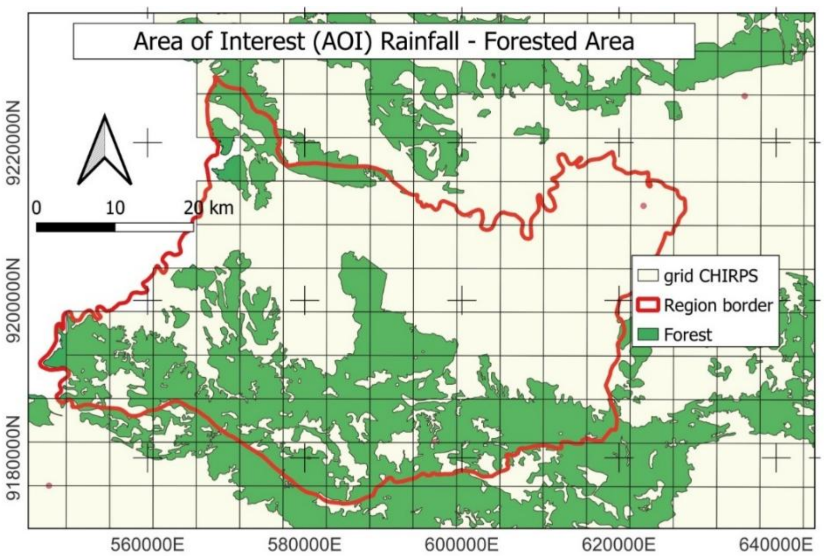

Figure 3. The position of grid cells and forest area in Bojonegoro Regency.
Source: Authors' processing

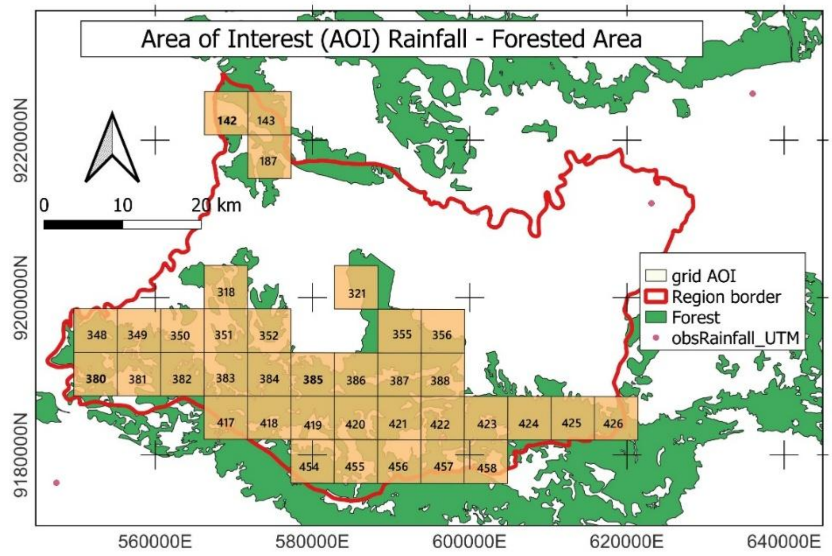

Figure 4. Grid number of NDVI based on precipitation grid.
Source: Authors' processing (2024)

Higher NDVI values indicate dense, healthy vegetation, while lower or negative values signify sparse vegetation or barren land. NDVI is closely associated with the fraction of Absorbed Photosynthetically Active Radiation (fAPAR) and chlorophyll content. NDVI values were then summarised using zonal means, medians, and maximum within 0.05 ° x 0.05 ° grid cells. The zonal NDVI grids matched the spatial resolution and alignment with the CHIRPS precipitation dataset.

The correlation between NDVI and precipitation was analysed using Pearson's Product-Moment Correlation (PPMC). NDVI values were compared with CHIRPS-corrected precipitation data at multiple time lags to assess temporal dependencies. As a parametric test, PPMC required normally distributed data. Therefore, precipitation values were first standardised using the Z-score transformation.

Linear regression was applied to assess potential causal relationships between NDVI and Rainfall. NDVI and standardised (Z-score) rainfall values were alternately used as dependent and independent variables. The analysis included two regression models:

a. NDVI as the dependent variable (Y), with Z-score Rainfall from previous months (lag-) as the independent variable.

b. Z-score Rainfall from subsequent months (lag+) as the dependent variable (Y), with NDVI as the independent variable.

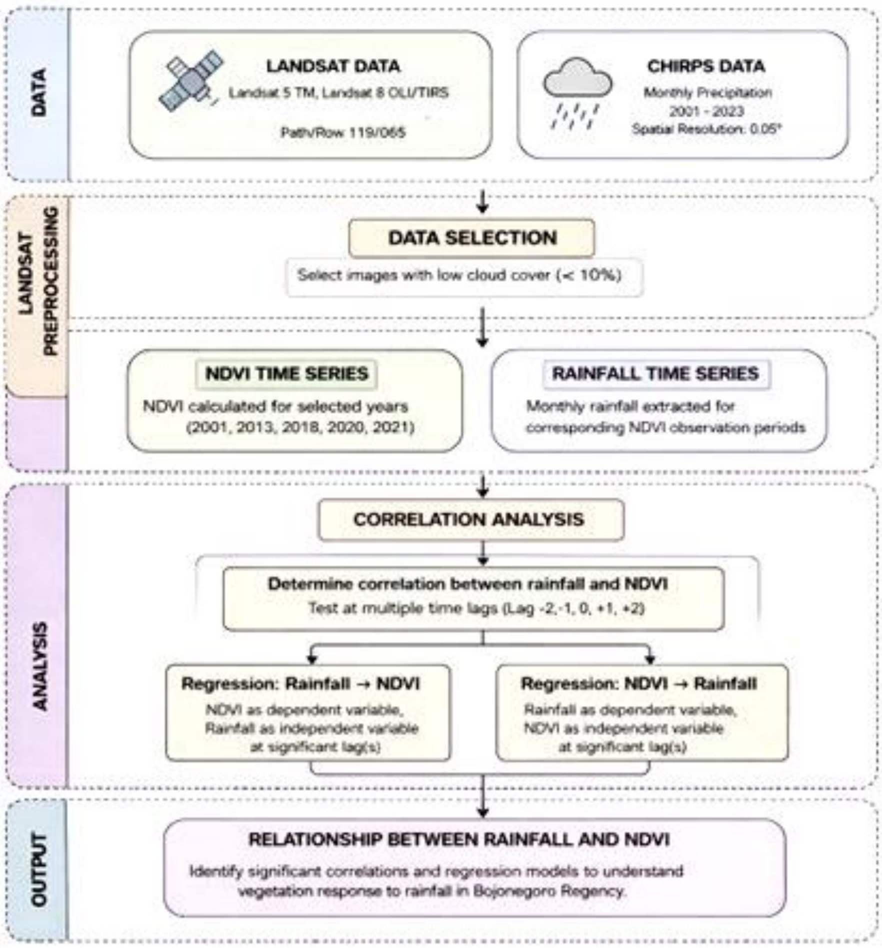

Figure 5. Research data and method flow.
Source: Authors' processing (2024)

Simple linear regression was used to examine the relationship between variables and was expressed as:

$$Y = \beta_0 + \beta_1 X \quad (2)$$

where Y is the dependent variable, X is the independent variable, β_0 is the intercept, and β_1 is the slope (beta coefficient).

The standard error of the slope (se) was calculated using the following formula:

$$se = \frac{\sqrt{\frac{\Sigma(Y_{obs} - Y_{pred})^2}{N-2}}}{\sqrt{\Sigma(X-\bar{X})^2}} \quad (3)$$

where Y_{obs} is the observed dependent value, Y_{obs} is the predicted dependent value, X is the independent variable, $\bar{X}$ is the mean of the independent variable, and N is the number of observations.

The confidence interval (CI) for the slope was calculated as:

$$CI = \beta_1 \pm t_{(n-1,\frac{\alpha}{2})} \frac{se}{\sqrt{N}} \quad (4)$$

where β_1 is the slope, $t_{(n-1,\frac{\alpha}{2})}$ is the critical t-value for *n-1* degrees of freedom and significance level α; *se* is the standard error of the slope, and *N* is the total number of observations. The research flow diagram is shown in **Figure 5**.

RESULTS AND DISCUSSION

1. Vegetation Index Changes

   a. Seasonal Change of NDVI

NDVI values were relatively low in 2001 (**Figure 6a**), with the lowest values in the northern forests and the highest in the south. A similar pattern was observed in 2023. Seasonal variations influence NDVI levels. At the end of the rainy season (May 2018), NDVI was higher, ranging from 0.263 to 0.402 (**Figure 6c**). In contrast, during the onset of the rainy season (October 2013), NDVI values were lower, mostly between 0.201 and 0.260 (**Figure 6b**). The highest NDVI values were consistently found in the south region, regardless of the season.

NDVI values were higher in April than in May. In April 2021, NDVI ranged from 0.401 to 0.468, with a minimum of 0.344. In May 2023, values ranged from 0.306 to 0.429, with most values between 0.388 and 0.429. Higher precipitation in April sustains vegetation with stable NDVI values, typically in groundwater-accessible recharge areas. Such areas, especially in the southern recharge zone, consistently exhibit high NDVI values in both early and late rainy seasons. Regions with lower precipitation tend to have more fluctuating NDVI values, indicating interdependence between forest cover and precipitation.

Table 1 shows that most grids experienced positive change during 2013, which means better vegetation health. However, one-third of these regions experienced a negative change. These regions are represented by grid numbers 355, 356, 382, 417, 418, 419, 420, 454, 455, 456, 457, 458, with the highest negative change positioned on grid 454 with 11.35% change relative to 2001. Besides, grids 455 and 455 experienced a 5.00 – 7.18% decline in NDVI relative to 2001. Both grids are mostly barren land or forest that has been cleared for agricultural activity.

Despite the negative change that occurred from 2001 to 2013, by 2018, there was a similar positive trend for the entire region. The forest located in the northern region experienced the largest positive trend up to 25.83% from the base time 2001. These positive trends remained until May 2023. Between 2018 and 2023, 2021 showed the largest positive change, ranging from 9.77% up to 31.57%, with a median 20.13%. After a slight change during 2021, NDVI showed a relatively small positive change from the base period. During 2023, there is a negative change relative to 2021. However, compared to NDVI 2018, the change in 2023 remains positive.

The results indicated that NDVI values were generally higher during the peak and end of the rainy season compared to their onset. Soil water-holding capacity remained adequate to support vegetation growth at the end of the rainy season. As a result, the NDVI reached its maximum during this period (Zhang et al., 2018). However, during the early rainy season, limited Rainfall often resulted in a negative water balance. Continuous lack of water adversely affected plant health. Forest ecosystems are sensitive to dry conditions, as reflected by the decline in NDVI during the dry season (Zhang et al., 2016).

Areas exhibiting negative NDVI may be related to degraded or converted land. During the dry season (June – September), crops often fail to grow. Due to these sudden land cover changes, NDVI fluctuations are more pronounced in these converted areas (**Figure 6b**). Regions dominated by natural or production forests generally show more stable NDVI values. Forested areas function as groundwater recharge zones, which help to retain subsurface moisture levels. However, forest conversion leads to increased surface evaporation. Regions with highly fluctuating NDVI values are likely experiencing the most significant forest cover changes (Erasmi et al., 2009). In contrast, stable NDVI values represent undisturbed forest ecosystems.

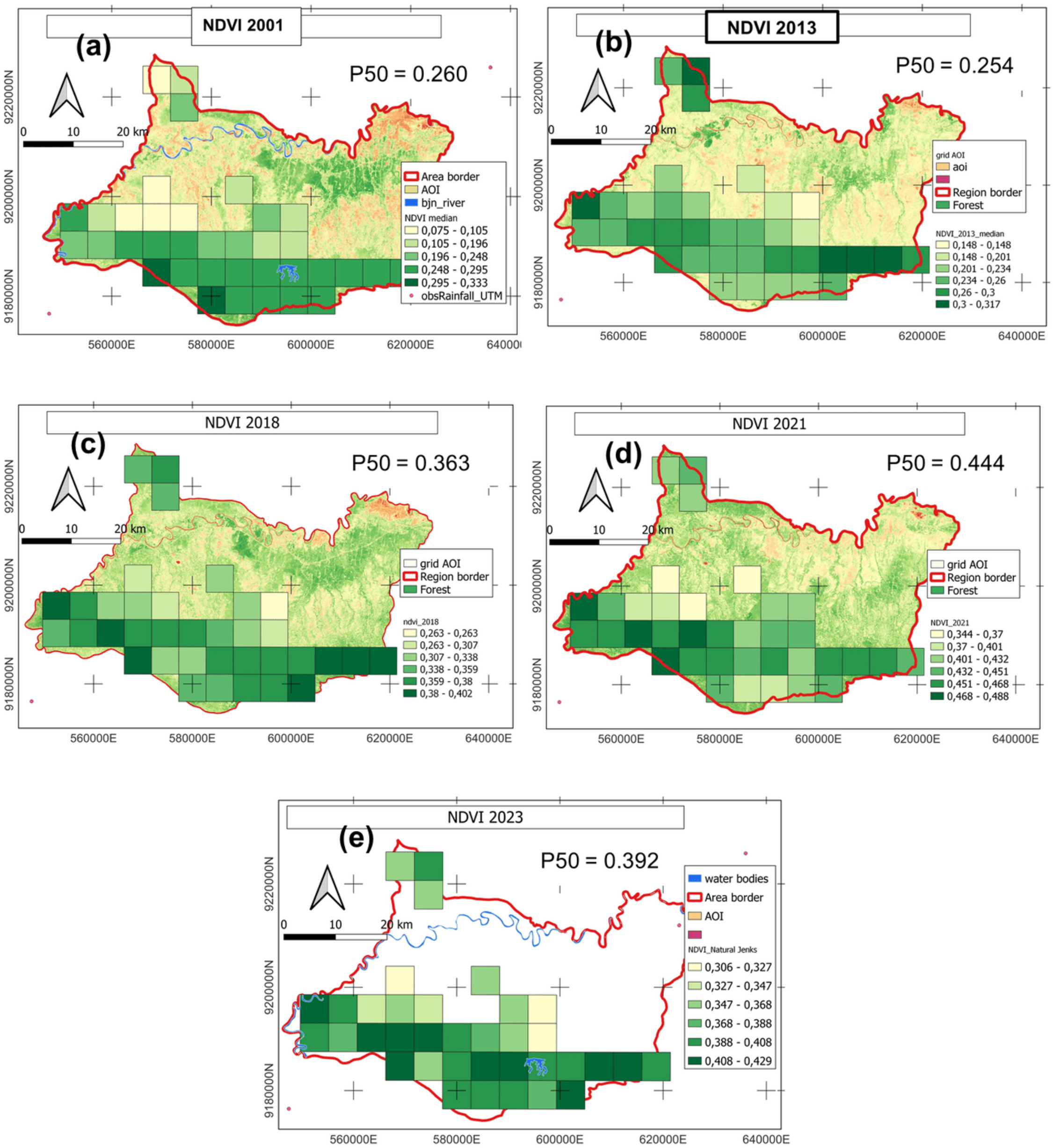

Figure 6. Median NDVI (a) 2008; (b) 2013; (c) 2018; (d) 2021; (e)2023.

Source: Research Analysis (2024)

Table 1. Percent of change (%) zonal median NDVI from the base period year 2001

Grid number	**Year**			
	2001-2013 (%)	**2001-2018 (%)**	**2001-2021 (%)**	**2001-2023 (%)**
142	16.82	25.83	31.57	26.58
143	13.68	19.16	26.42	21.60
187	6.22	12.31	20.36	13.56
318	13.55	23.15	29.09	24.41
321	5.79	18.76	22.68	20.92
348	2.75	11.07	19.08	13.92
349	6.18	18.39	25.19	20.95
350	14.00	24.29	28.57	24.89
351	13.25	21.55	29.09	24.21
352	12.49	18.20	24.15	22.70
355	-2.75*	11.14	20.63	14.19
356	-1.40*	10.14	24.93	14.76
380	2.06	12.91	23.87	16.18
381	0.95	12.34	22.61	14.62
382	-1.33*	9.37	19.27	13.00
383	0.66	9.84	19.05	13.44
384	2.65	12.19	21.74	15.81
385	1.12	11.73	21.27	14.58
386	4.58	13.09	21.61	16.63
387	2.16	14.23	25.12	15.32
388	2.15	12.82	26.70	13.39
417	-4.65*	5.89	14.59	8.22
418	-2.49*	5.07	18.14	7.59
419	-4.74*	4.08	17.14	10.30
420	-2.08*	10.18	17.09	13.84
421	3.08	11.30	19.90	15.10
422	1.72	10.18	16.43	12.27
423	3.32	10.04	17.75	12.83
424	3.50	11.26	18.21	12.88
425	2.69	11.23	17.67	12.80
426	2.53	11.75	17.48	12.83
454	-11.35*	2.53	12.41	6.79
455	-7.18*	5.91	9.77	9.75
456	-5.03*	9.62	12.97	12.27
457	-3.92*	10.13	15.61	11.88
458	-1.16*	11.37	16.97	14.04
Min	-11.35	2.53	9.77	6.79
Max	16.82	25.83	31.57	26.58
Median	2.15	11.34	20.13	13.98

Source: Research Analysis, 2024

Areas exhibiting negative NDVI trends are typically those where forests have been converted or degraded. During the dry season (June–September), crops often fail to grow. Due to these sudden land cover changes, NDVI fluctuations are more pronounced in these converted areas (**Figure 6b**). Regions dominated by natural or production forests generally show more stable NDVI values. Forested areas function as groundwater recharge zones, which help to retain subsurface moisture levels. However, forest conversion leads to increased surface evaporation. Regions with highly fluctuating NDVI values are likely experiencing the most significant forest cover changes (Erasmi et al., 2009). In contrast, stable NDVI values represent undisturbed forest ecosystems.

b. Interannual Maximum NDVI Dynamics

Figure 7 shows the maximum NDVI fluctuations from 2001 to 2023. The lowest maximum value appeared in 2001 (**Figure 7a**), while the highest value appeared in 2021 (**Figure 7d**). Vegetation characteristics in 2001 and 2018 were similar. In 2013, 47% of the grid had maximum NDVI values between 0.500 and 0.600. In 2018, 50% of the grid showed values in the same range. **Figure 7d** showed that the NDVI peak occurred in 2021. About 40% of the grid reached maximum NDVI values between 0.600 and 0.700. All grids had vegetation indices above 0.500.

Vegetation index fluctuations were also linked to interannual climate phenomena such as ENSO and IOD. Severe drought in 1997/1998, followed by high Rainfall during the 2000 La Niña, led to low NDVI values in 2001. The year 2001 marked a recovery from these extreme events. El Niño and a strong positive Indian Ocean Dipole in 1997/1998 caused extreme drought (Mulyanti, 2023), widespread forest fires, and vegetation stress. Forest vegetation likely recovered between 2001 and 2024. The dynamic of vegetation after severe drought in 2015 and heavy Rainfall in 2016 showed by 2018 (**Figure 7c**). This event had less impact than the 1997–2000 period. Southern areas (grid 417 to grid 458) showed similar maximum NDVI values between 0.400 and 0.500.

The years 2020 to 2021 were known as wet years, marked by intense convection and cloud formation across the tropics. In Java Island, this condition resulted from complex and continuous or coincidental interactions between several coincidental phenomena, including a moderate negative Indian Ocean Dipole (IOD), moderate La Niña, Madden-Julian Oscillation (MJO), and tropical waves (Lubis et al., 2022). A negative IOD contributed to increased Rainfall in Java (Hermawan, 2018; Tejavath et al., 2024). Plants that received more Rainfall could optimise growth, capture sunlight, and assimilate soil carbon (Sun et al., 2020). In this case, the plant could reach its maximum.

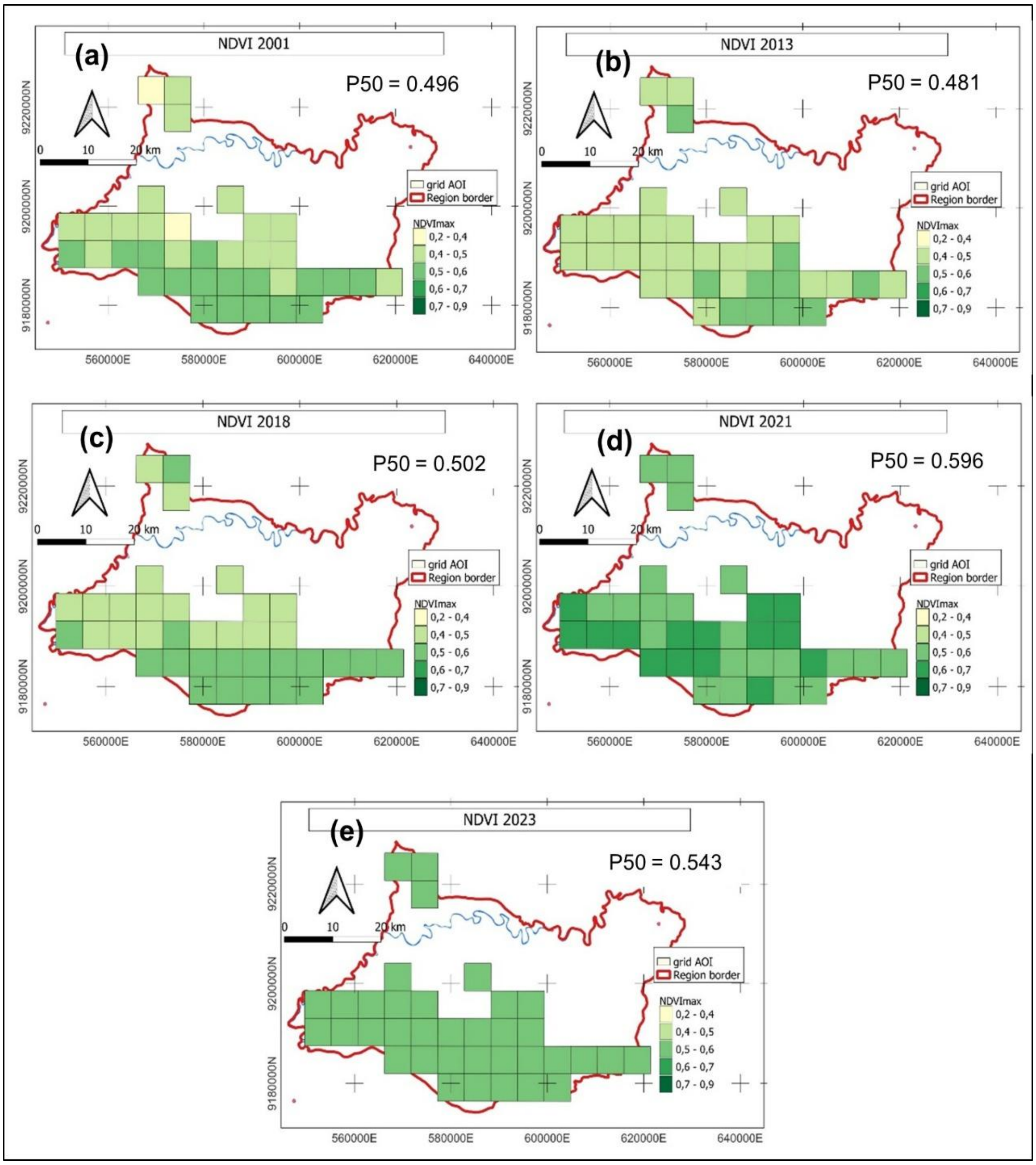

Figure 7. Maximum NDVI: (a) 2001; (b) 2013; (c) 2018; (d) 2021; (e)2023. P50 represents the median value of the entire NDVI value from each year.

Source: Research Analysis (2024)

Productive ecosystems generally have lower resilience to wet conditions (Hossain & Li, 2021). Vegetation shows resilience to drought but has limited resilience to excess moisture. Resilience refers to the ecosystem's ability to return to its original state after disturbance. One example occurred in 2018, which followed the severe 2015 drought associated with a strong El Niño event (Mulyanti et al., 2023; Santoso et al., 2017). Maximum NDVI values in 2001, 2013, and 2018 appeared similar, in contrast to 2021, which represented a wet year.

Conditions became stable by 2023. Maximum NDVI values reached uniform levels across all grids in 2023 (**Figure 7e**), within the 0.500–0.600 range. The difference between 2021 and 2023 showed that the system returned to its earlier condition. The NDVI increase in 2021 did not persist over time.

NDVI values increased from 2001 to 2023, with a median change of 13.98% relative to the 2001 baseline (**Table 1**). This result confirmed the previous findings (Furusawa et al., 2023) that reported a widespread increase in vegetation index across most parts of Indonesia. Their study used aggregate values at the regional scale, which meant smaller local NDVI declines did not affect the general trend.

Furusawa et al. (2023) also reported an NDVI increase in East Java Province. In general, the most significant NDVI changes occurred between 2005 and 2010. Vegetation was exposed to various types of climate variability and disturbances. These climate dynamics include droughts that caused NDVI to decline (Hossain & Li, 2021; Jiang et al., 2024; Vicente-Serrano et al., 2020), as well as wet conditions that led to rapid NDVI increases (Famiglietti et al., 2021). Under these conditions, vegetation develops adaptive responses to environmental change (Isbell et al., 2015). However, biodiversity loss driven by anthropogenic activity could reduce ecosystem stability and weaken its ability to recover productivity following climatic events (Isbell et al., 2015). These findings suggest that climate anomalies have short-term effects but do not alter the long-term NDVI trend.

Although Global Forest Watch (2024) recorded forest loss in Bojonegoro Regency, NDVI values increased from 2001 to 2020. The data indicated a net tree cover loss of 5.98 kha (–7.7%), including 2.51 kha of disturbed forest (Hansen et al., 2013). The primary cause of forest loss was the expansion of permaculture activities in forest areas, which were later classified as agroforestry. The conditions seem to contrast: NDVI values increasing, on the other hand, there is a loss of tree cover of about -7.7%. This difference could occur because NDVI measures horizontal vegetation changes rather than vertical attributes such as canopy height or growth. In agroforestry systems where trees and crops coexist, NDVI cannot capture the real problem. There is a need for a distinction between disturbed forest and undisturbed forest for assessing the NDVI value.

2. Relationship Between Precipitation and Vegetation Index

Table 2 showed a moderate-to-strong relationship between precipitation and NDVI during 2001. Precipitation and vegetation formed an interdependent hydrological system within the river basin. In 2001, the highest correlation (0.577) appeared at lag –1 (April), indicating that Rainfall in the previous month influenced NDVI. A similar value at lag –2 (March) suggested that March rainfall affected NDVI in May. No significant correlation was observed at lag 0 and lag +1, but a moderate-to-strong correlation reappeared at lag +2 (July). These results aligned with previous findings (Sun et al., 2020).

A positive correlation indicated that high precipitation corresponded with high NDVI. However, it was also possible that high NDVI contributed to increased precipitation. Historically, lags –1 and –2 may reflect the influence of Rainfall on vegetation, while lags +1 and +2 suggest that NDVI might act as an indicator of upcoming Rainfall. In October 2013, the NDVI–precipitation correlation was weak, ranging from –0.143 to 0.217. By May 2018, the relationship turned negative from lag 0 to lag –2, with the strongest negative value (–0.332) at lag –1 (April). This indicated that high Rainfall in April 2018 was associated with lower NDVI in May.

Table 2. Correlation coefficient (r) between Rainfall and NDVI for lag – 2 to lag+2

Year	**Month of lag-0**	**lag-2**	**lag-1**	**lag-0**	**lag+1**	**lag+2**
2001	May	**0.525**	**0.575**	0.076	-0.139	**0.455**
2013	Ocktober	0.186	-0.143	0.015	0.012	0.217
2018	May	-0.127	-0.332	0.062	0.165	0.310

Source: Research Analysis (2024)

Table 3. Regression between NDVI (y) and precipitation lag-1 (x) for a specific year

Year	Slope (β_1)	Standard Error (*se*)	Conf. Interval	P-value	Adjusted R^2	Model
2001	0.032	0.010	0.010, 0.054	0.005	0.207	Y = 0.229 + 0.032*(Zrainfall)
2013	-0.007	0.007	-0.021, 0.008	0.347	-0.003	Y = 0.254 -0.007*(Zrainfall)
2018	0.006	0.006	-0.344, 0.366	0.280	0.006	Y = 0.355 +0.006*(Zrainfall)

Source: Research Analysis (2024)

Table 4. Regression between rainfall at lag+2 (y) with NDVI (x) for specific year

Year	Slope (β_1)	Standard Error (*se*)	Conf. Interval	P-value	Adjusted R^2	Model
2001	6.410	2.152	2.036, 10.784	0.005	0.207	Y = -1.470 + 6.410*(NDVIl)
2013	5.280	4.074	-3.000, 13.561	0.204	0.019	Y = -1.342 -5.280*(NDVI)
2018	-0.882	5.255	-11.56, 9.798	0.867	-0.029	Y = 0.313 – 0.882*(NDVI)

Source: Research Analysis (2024)

Overall, the NDVI–precipitation relationship was complex. Although a moderate positive correlation appeared in 2001, a negative association was recorded in 2013 and 2018. A negative correlation meant that higher Rainfall was linked to lower NDVI, and vice versa. At the beginning of the rainy season in October, NDVI and precipitation showed minimal correlation. However, in May 2018, the correlation was negative at lag –1 but turned positive (0.310) at lag +2. This implied that NDVI in May correlated with Rainfall two months later. For example, NDVI in May 2001 showed a positive correlation with July 2001 rainfall. July marked the dry season in the monsoonal climate region.

These findings indicate that neither Rainfall nor NDVI reliably captures a direct or causal relationship. Across the three observed years, only **2001** produced a model with statistically significant results. The regression analysis in 2001 showed a meaningful relationship and suggested causal links between Rainfall and NDVI. However, for **2013** and **2018**, the relationship appeared too complex to be explained by a simple linear model.

Despite the moderate correlation observed in 2018, there was limited evidence to support a clear causal relationship between Rainfall and NDVI.

As shown in **Table 3**, the regression analysis using Rainfall as the independent variable and NDVI as the dependent variable produced a p-value greater than 0.05 and an adjusted R^2 of –0.006, indicating a weak model. A similar result appeared in **Table 4**, where NDVI at lag 0 served as the independent variable, and Rainfall at lag +2 was the dependent variable. In this case, the standard error of the beta coefficient exceeded the coefficient itself. With a p-value above 0.05 and an adjusted R^2 of –0.029, the model lacked predictive power and was not statistically valid.

Statistical significance was observed between rainfall and NDVI in 2001. In contrast, weak or inconsistent correlations were found in 2013 and 2018. These correlation patterns were confirmed by regression analyses shown in **Figure 8**. Only the 2001 data could be explained by the regression model, while the 2013 and 2018 results could not be adequately modelled.

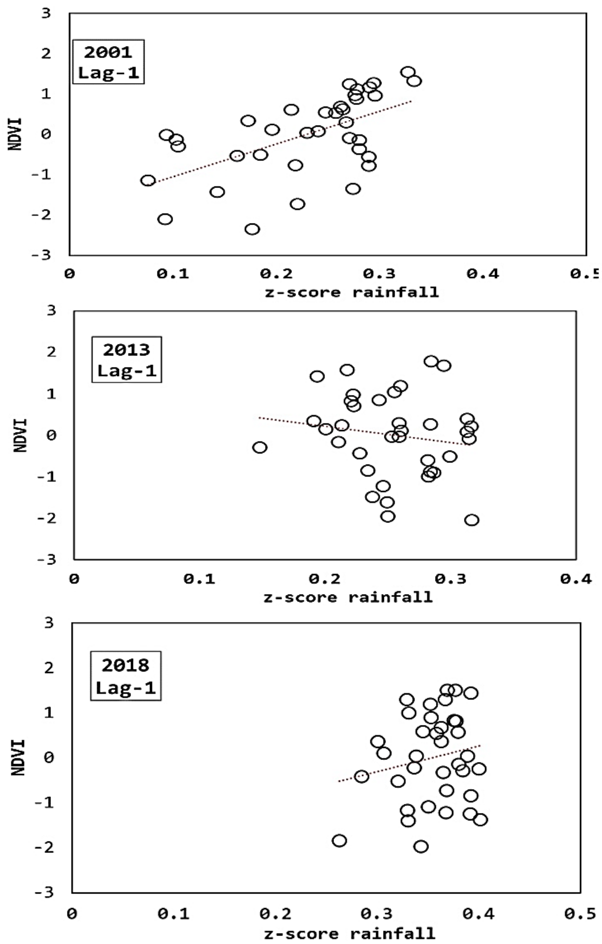

Figure 8. Scatter plot rainfall (lag-1) with NDVI: (a) 2001; (b) 2013; (c) 2018.
Source: Research Analysis (2024)

3. Discussion

NDVI in Bojonegoro shows a clear seasonal variation. NDVI is higher at the end of the rainy season than at the beginning. This pattern indicates that vegetation responds to accumulated Rainfall rather than immediate precipitation. Rainfall at the beginning of the season is still limited because soil moisture is not sufficient to support optimal growth. This result confirms that NDVI response to Rainfall involves a time lag.

The relationship between NDVI and Rainfall is not consistent across years. Significant correlation appears only in 2001, at lag –2, lag –1, and lag +2. This result shows that Rainfall one to two months before affects NDVI, and NDVI may also relate to Rainfall in subsequent months. In contrast, no clear relationship appears in 2013 and 2018, except during lag+2. This finding does not fully agree with previous studies that report stable positive correlations between NDVI and precipitation (Campos et al., 2021; Garai et al., 2022; Sa'adi et al., 2024). This difference suggests that Rainfall alone does not control vegetation dynamics in this region. Other factors, such as land cover condition and previous climate events, likely influence NDVI variability.

NDVI reaches the highest value in 2021, which corresponds to a wet year. However, this increase does not persist, as NDVI returns to moderate levels in 2023. This pattern indicates that vegetation responds rapidly to favorable conditions but does not maintain high productivity over time. A similar response appeared in 2018 after the 2015 drought. NDVI values in 2018 are comparable to those in 2001 and 2013. This result suggests that forest vegetation in the study area has the capacity to recover after short-term climate disturbance.

Spatial patterns also support this interpretation. NDVI remains more stable in forest-dominated areas but fluctuates in converted or degraded land. The negative NDVI observed in October 2013 likely reflects degraded forest or transitional land use. This finding is consistent with previous studies showing that natural forests are less sensitive to climate variability than cropland or degraded land (Erasmi et al., 2009; Ghebrezgabher et al., 2020). Forest systems maintain soil moisture and reduce the impact of rainfall variability.

Over the long term, NDVI increases by 13.98% from 2001 to 2023. This trend is consistent with a previous study, which reports increasing NDVI across Indonesia (Furusawa et al., 2023). However, strong interannual variation is still observed. Climate anomalies such as drought and wet events affect NDVI in the short term but do not alter the overall trend. This result indicates that vegetation adapts to climate variability, although continued land cover change may reduce ecosystem stability and recovery capacity.

NDVI reflects vegetation dynamics within the growth cycle and is influenced by fluctuations in precipitation and temperature. Extended high-rainfall periods, characterised by consecutive wet days, enable optimal cell growth. However, water scarcity slows growth, and when combined with high temperatures, increased transpiration accelerates water loss from plants. High NDVI values indicate dense and healthy vegetation (Zhou & Wang, 2011). NDVI values approaching 1.00 suggest areas dominated by vigorous plant cover, while low or negative NDVI values signal environmental degradation due to deforestation or land conversion to non-vegetated use (Zhang et al., 2021).

Forests act as protective buffers that mitigate drought risks (Staal et al., 2018). With the rise of forest conversion, the risk of precipitation losses increased, resulting in drought risk. A 1% decrease in forest cover results in a monthly rainfall reduction of approximately 0.25 mm (Smith et al., 2023). Although reduced precipitation affects NDVI, deforestation also directly decreases Rainfall and potential evapotranspiration, which in turn increases surface runoff (Ma et al., 2024). Moreover, in the case of hilly topography like the study area, there is a flash flood hazard.

This study has several limitations. NDVI represents vegetation greenness and does not directly correspond to land use or vegetation structure, so validation using land use data is limited. Field-based validation is not conducted, which may affect interpretation, especially in agroforestry areas. Some years are not fully captured due to cloud cover, which reduces temporal consistency.

Future studies should include field observations to improve NDVI validation, especially in agroforestry areas with complex vegetation structure.

The use of higher temporal resolution or multi-source satellite data is also needed to reduce gaps caused by cloud cover. In addition, continuous time series analysis should be applied to better capture lag effects between rainfall and vegetation response. Integration of NDVI with land cover change analysis is important to explain how forest conversion influences vegetation dynamics under climate variability.

The study highlights that forests could maintain stable NDVI even during high variability of precipitation. Degraded forest and forest conversion caused a less resilient ecosystem to climate-related hazards. Planned management is needed to stabilize the ecosystem for future climate change.

CONCLUSIONS

NDVI exhibits both seasonal and interannual variation. In monsoonal regions such as Bojonegoro, NDVI values are generally higher at the end of the rainy season than at the beginning. The median NDVI at the end of the rainy season is 0.365, compared to 0.254 at the beginning. The highest maximum NDVI was recorded in 2021, with a median value of 0.596. Forested areas show greater stability in response to climate variability than croplands or degraded land. The negative NDVI change observed in October 2013 is likely associated with forest degradation.

The relationship between rainfall and NDVI is complex and inconsistent, with a significant correlation observed only in 2001. During that year, NDVI correlated with precipitation at lags –2, –1, and +2, suggesting that Rainfall one to two months prior can influence current NDVI, and NDVI may also correspond to Rainfall two months later.

This analysis is regional, reflecting spatial averages rather than localized interactions. A finer-scale spatial analysis would require time series data of both NDVI and precipitation. In agroforestry regions, NDVI analysis alone is insufficient. Field observations and ground validation are necessary to assess the accuracy of NDVI-based vegetation assessments. Planned management is needed to stabilize the forest ecosystem for future climate change.

ACKNOWLEDGMENTS

LPPM Universitas Bojonegoro funded the study.

REFERENCES

Campos, B. O. O., Paredes, F., Rey, J. C., Lobo, D., & Galvis-Causil, S. (2021). The relationship between the normalized difference vegetation index, Rainfall, and potential evapotranspiration in a banana plantation of Venezuela. *SAINS TANAH - Journal of Soil Science and Agroclimatology*, *18*(1), Article 1. https://doi.org/10.20961/stjssa.v18i1.50379

Carvalho, S., Oliveira, A., Pedersen, J. S., Manhice, H., Lisboa, F., Norguet, J., de Wit, F., & Santos, F. D. (2020). A changing Amazon rainforest: Historical trends and future projections under post-Paris climate scenarios. *Global and Planetary Change*, *195*, 103328. https://doi.org/10.1016/j.gloplacha.2020.103328

Congedo, L. (2021). Semi-Automatic Classification Plugin: A Python tool for the download and processing of remote sensing images in QGIS. *Journal of Open Source Software*, *6*(64), 3172. https://doi.org/10.21105/joss.03172

Erasmi, S., Propastin, P., Kappas, M., & Panferov, O. (2009). Spatial Patterns of NDVI Variation over Indonesia and Their Relationship to ENSO Warm Events during the Period 1982–2006. *Journal of Climate*, *22*(24), 6612–6623. https://doi.org/10.1175/2009JCLI2460.1

Famiglietti, C. A., Michalak, A. M., & Konings, A. G. (2021). Extreme wet events as important as extreme dry events in controlling spatial patterns of vegetation greenness anomalies. *Environmental Research Letters*, *16*(7), 074014. https://doi.org/10.1088/1748-9326/abfc78

Funk, C., Peterson, P., Landsfeld, M., Pedreros, D., Verdin, J., Shukla, S., Husak, G., Rowland, J., Harrison, L., Hoell, A., & Michaelsen, J. (2015). The climate hazards infrared precipitation with stations—A new environmental record for monitoring extremes. *Scientific Data*, *2*(1), Article 1. https://doi.org/10.1038/sdata.2015.66

Furusawa, T., Koera, T., Siburian, R., Wicaksono, A., Matsudaira, K., & Ishioka, Y. (2023). Time-series analysis of satellite imagery for detecting vegetation cover changes in Indonesia. *Scientific Reports*, *13*(1), 8437. https://doi.org/10.1038/s41598-023-35330-1

Garai, S., Khatun, M., Singh, R., Sharma, J., Pradhan, M., Ranjan, A., Rahaman, S. M., Khan, M. L., & Tiwari, S. (2022). Assessing correlation between Rainfall, normalized difference Vegetation Index (NDVI) and land surface temperature (LST) in Eastern India. *Safety in Extreme Environments*, *4*(2), 119–127. https://doi.org/10.1007/s42797-022-00056-2

Ghebrezgabher, M. G., Yang, T., Yang, X., & Eyassu Sereke, T. (2020). Assessment of NDVI variations in responses to climate change in the Horn of Africa. *The Egyptian Journal of Remote Sensing and Space Science*, *23*(3), 249–261. https://doi.org/10.1016/j.ejrs.2020.08.003

Hansen, M. C., Potapov, P. V., Moore, R., Hancher, M., Turubanova, S.

A., Tyukavina, A., Thau, D., Stehman, S. V., Goetz, S. J., Loveland, T. R., Kommareddy, A., Egorov, A., Chini, L., Justice, C. O., & Townshend, J. R. G. (2013). High-Resolution Global Maps of 21st-Century Forest Cover Change. *Science*, *342*(6160), 850–853. https://doi.org/10.1126/science.1244693

Hermawan, E. (2018). Impact of teleconnection between Indian Ocean Dipole (IOD) and El Niño at normal (neutral) phase condition on the Java Monsoon rainfall variability. *Journal of Physics: Conference Series*, *1130*(1), 012038. https://doi.org/10.1088/1742-6596/1130/1/012038

Hossain, M. L., & Li, J. (2021). NDVI-based vegetation dynamics and its resistance and resilience to different intensities of climatic events. *Global Ecology and Conservation*, *30*, e01768. https://doi.org/10.1016/j.gecco.2021.e01768

Isbell, F., Craven, D., Connolly, J., Loreau, M., Schmid, B., Beierkuhnlein, C., Bezemer, T. M., Bonin, C., Bruelheide, H., de Luca, E., Ebeling, A., Griffin, J. N., Guo, Q., Hautier, Y., Hector, A., Jentsch, A., Kreyling, J., Lanta, V., Manning, P., … Eisenhauer, N. (2015). Biodiversity increases the resistance of ecosystem productivity to climate extremes. *Nature*, *526*(7574), 574–577. https://doi.org/10.1038/nature15374

Jiang, L., Liu, B., Guo, H., Yuan, Y., Liu, W., & Jiapaer, G. (2024). Assessing vegetation resilience and vulnerability to drought events in Central Asia. *Journal of Hydrology*, *634*, 131012. https://doi.org/10.1016/j.jhydrol.2024.131012

Landsat Science Outreach Team. (2023, June 15). *Landsat 7—NASA Science*. https://science.nasa.gov/mission/landsat-7/

Lawrence, D., & Vandecar, K. (2015). Effects of tropical deforestation on climate and agriculture. *Nature Climate Change*, *5*(1), 27–36. https://doi.org/10.1038/nclimate2430

Lubis, S. W., Hagos, S., Hermawan, E., Respati, M. R., Ridho, A., Risyanto, Paski, J. A. I., Muhammad, F. R., Siswanto, Ratri, D. N., Setiawan, S., & Permana, D. S. (2022). Record-Breaking Precipitation in Indonesia's Capital of Jakarta in Early January 2020 Linked to the Northerly Surge, Equatorial Waves, and MJO. *Geophysical Research Letters*, *49*(22), e2022GL101513. https://doi.org/10.1029/2022GL101513

Ma, S., Zhou, S., Yu, B., & Song, J. (2024). Deforestation-induced runoff changes dominated by forest-climate feedbacks. *Science Advances*, *10*(33), eadp3964. https://doi.org/10.1126/sciadv.adp3964

Marga, M., Indarto, I., Nevila, R. N., Andi, S. A., & Lukman, H. F. (2024). Land use and land cover change in East Java from 2015 to 2021: Use optical imagery and Google Earth engine. *Environmental & Socio-Economic Studies*, *12*(1), 69–80.

https://doi.org/10.2478/environ-2024-0007

Mulyanti, H. (2022). Identifikasi Wilayah Hujan Di Kabupaten Bojonegoro Menggunakan Teknik Klaster Aglomerasi: *Jurnal Teknik Sipil*, *7*(2), Article 2. https://doi.org/10.56071/deteksi.v7i2.396

Mulyanti, H. (2023). Keterkaitan Antara El NiÃ±o-Southern Oscillation (ENSO) Dengan Variabilitas Curah Hujan Bojonegoro. *Berkala Ilmiah Pertanian*, *6*(1), Article 1. https://doi.org/10.19184/bip.v6i1.37221

Mulyanti, H., Istadi, I., & Gernowo, R. (2023). Historical, Recent, and Future Threat of Drought on Agriculture in East Java, Indonesia: A Review. *E3S Web of Conferences*, *448*, 03016. https://doi.org/10.1051/e3sconf/202344803016

Sa’adi, Z., Alias, N. E., Yusop, Z., Mazilamani, L. S., Houmsi, M. R., Houmsi, L. N., Shahid, S., Aris, A., Ramli, M. W. A., Khan, N., & Shukla, P. (2024). Examining the NDVI-Rainfall Relationship Under High Enso Event Influence Using Geographically Weighted Regression in Peninsular Malaysia. *IGARSS 2024 - 2024 IEEE International Geoscience and Remote Sensing Symposium*, 1908–1913. https://doi.org/10.1109/IGARSS53475.2024.10642469

Santoso, A., Mcphaden, M. J., & Cai, W. (2017). The Defining Characteristics of ENSO Extremes and the Strong 2015/2016 El Niño. *Reviews of Geophysics*, *55*(4), 1079–1129. https://doi.org/10.1002/2017RG000560

Smith, C., Baker, J. C. A., & Spracklen, D. V. (2023). Tropical deforestation causes large reductions in observed precipitation. *Nature*, *615*(7951), 270–275. https://doi.org/10.1038/s41586-022-05690-1

Staal, A., Tuinenburg, O. A., Bosmans, J. H. C., Holmgren, M., van Nes, E. H., Scheffer, M., Zemp, D. C., & Dekker, S. C. (2018). Forest-rainfall cascades buffer against drought across the Amazon. *Nature Climate Change*, *8*(6), 539–543. https://doi.org/10.1038/s41558-018-0177-y

Sun, G., Guo ,Bing, Zang ,Wenqian, Huang ,Xiangzhi, Han ,Baomin, Yang ,Xiao, Chen ,Shuting, Wei ,Cuixia, & and Wu, H. (2020). Spatial–temporal change patterns of vegetation coverage in China and its driving mechanisms over the past 20 years based on the concept of geographic division. *Geomatics, Natural Hazards and Risk*, *11*(1), 2263–2281. https://doi.org/10.1080/19475705.2020.1837967

Tejavath, C. T., Ashok, K., Chakraborty, S., & Pentakota, S. (2024). Indian Ocean Dipole Variations During the Last Millennium in PMIP3 Simulations. *Geophysical Research Letters*, *51*(16), e2024GL110112. https://doi.org/10.1029/2024GL110112

Vicente-Serrano, S. M., Quiring, S. M., Peña-Gallardo, M., Yuan, S., & Domínguez-Castro, F. (2020). A review of environmental droughts:

Increased risk under global warming? *Earth-Science Reviews*, *201*, 102953. https://doi.org/10.1016/j.earscirev.2019.102953

Weiskopf, S. R., Rubenstein, M. A., Crozier, L. G., Gaichas, S., Griffis, R., Halofsky, J. E., Hyde, K. J. W., Morelli, T. L., Morisette, J. T., Muñoz, R. C., Pershing, A. J., Peterson, D. L., Poudel, R., Staudinger, M. D., Sutton-Grier, A. E., Thompson, L., Vose, J., Weltzin, J. F., & Whyte, K. P. (2020). Climate change effects on biodiversity, ecosystems, ecosystem services, and natural resource management in the United States. *Science of The Total Environment*, *733*, 137782. https://doi.org/10.1016/j.scitotenv.2020.137782

Zhang, Y., Migliavacca, M., Penuelas, J., & Ju, W. (2021). Advances in hyperspectral remote sensing of vegetation traits and functions. *Remote Sensing of Environment*, *252*, 112121. https://doi.org/10.1016/j.rse.2020.112121

Zhang, Y., Wang, X., Li, C., Cai, Y., Yang, Z., & Yi, Y. (2018). NDVI dynamics under changing meteorological factors in a shallow lake in future metropolitan, semiarid area in North China. *Scientific Reports*, *8*(1), 15971. https://doi.org/10.1038/s41598-018-33968-w

Zhang, Y., Zhu, Z., Liu, Z., Zeng, Z., Ciais, P., Huang, M., Liu, Y., & Piao, S. (2016). Seasonal and interannual changes in vegetation activity of tropical forests in Southeast Asia. *Agricultural and Forest Meteorology*, *224*, 1–10. https://doi.org/10.1016/j.agrformet.2016.04.009

Zhou, X., & Wang, Y.-C. (2011). Spatial–temporal dynamics of urban green space in response to rapid urbanization and greening policies. *Landscape and Urban Planning*, *100*(3), 268–277. https://doi.org/10.1016/j.landurbplan.2010.12.013